

Soft switched Synchronous Boost Converter for Battery Dischargers

Zhiyong Dong^{1*}, and Gyubum Joung¹

^{1*}PhD student, ¹Professor, Energy and Electrical Engineering, Woosuk University, Korea

^{1*}120112296@stu.woosuk.ac.kr, ¹gbjoung@woosuk.ac.kr

Abstract

In this paper, we proposed a soft switched synchronous boost converter, which can perform discharging the battery, is proposed. The proposed converter has low switching loss even at high frequency operation due to its soft switching characteristics. The converter operates in synchronous mode to minimize conduction loss because of changing the rectified diode to MOSFET with a low on resistance. In this reason, the efficiency of the converter can be greatly improved in high frequency. In this paper, the battery discharger with a switching frequency of 100 kHz, has been designed. The designed converter also simulated to prove the converter's characteristics of synchronous operation as well as soft switching operation. The simulation shows that the proposed converter always meets the soft switching conditions of turning on and off switching in the zero voltage and zero current states. Therefore, simulation results have confirmed that the proposed battery discharge had soft switching characteristics. The simulation results have confirmed that the proposed battery discharger had soft switching and synchronous operation characteristics.

Keywords: Soft switched converter, Synchronous converter, Low switching loss, Battery discharger

1. Introduction

Most converters used in industry use pulse width modulation (PWM) converters [1]. For moving objects such as automobiles, satellites and airplanes, it is very important that converters minimize weight and volume. To minimize the weight and volume of converters, filters consisting of inductors and capacitors should be minimized, as these filters account for much of the weight and volume of converters [2]. Therefore, in order to minimize the weight and volume of the converter, the converter must be operated at a high switching frequency. Thus, resonant converters were proposed for high frequency switching operations [3]. The resonant converter has the disadvantage of having a low switching loss, but increasing conduction loss for operation of the resonant circuit [4-6]. Meanwhile, there have been many studies on soft switching PWM converters that can reduce conduction losses of resonant converters [7]. However, these methods have a disadvantage of having a conduction loss of the converter due to the voltage drop of the diode. In addition, a soft-switched synchronous Buck converter used for battery charging is being utilized to reduce the conductive loss of diodes [8-10].

In this study, a synchronous Boost converter with soft switching is proposed. The proposed soft switching synchronous Boost converter has very low switching losses due to its soft switching characteristics. Also, the synchronous operation of the converter greatly reduces the conduction loss. Therefore, switching loss and

conduction loss are very low even in the high frequency operation of the converter and may have high efficiency characteristics. High frequency switching operation of converter minimizes size and weight. In this paper, the proposed converter was used for battery discharge. In addition, the proposed converter was analyzed, designed and simulated through piecewise linear electrical circuit simulation (PLECS) software. Simulation results indicate that the proposed battery discharger has soft switching and synchronization characteristics during operating mode. We also simulated the transient response of the designed converter. The results show that the converter responds to discharge current commands quickly within 0.05 ms.

2. High efficiency proposed converter

Figure 1 shows a proposed converter with a Boost type synchronous converter in which the switch operates at zero current or zero voltage with switching operation. In Figure 1, the inductance of the saturated inductor L_S is L_{S1} when the inductor is saturated and L_{S2} in the inductance of inductor when the inductor is not saturated. The saturation current of the inductor L_S is assumed to be I_{LS} . C_r and L_r are resonant capacitor and inductor.

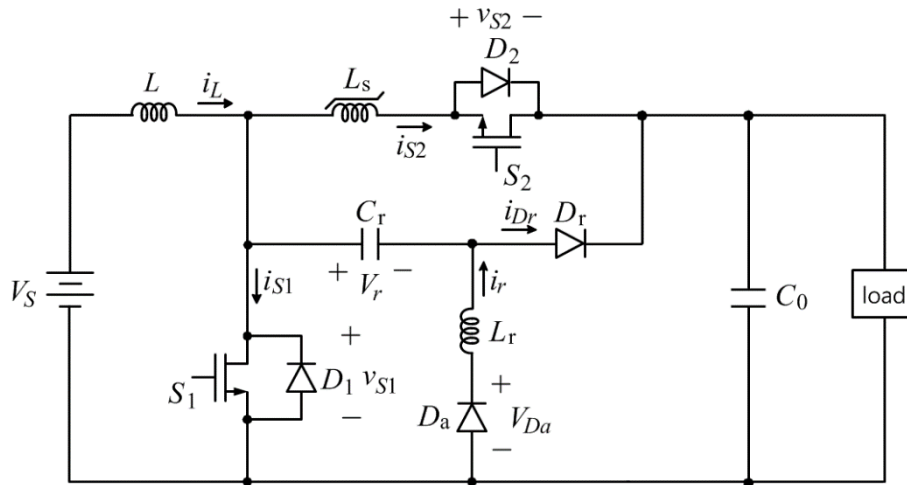


Figure 1. Proposed boost converter

Figure 2 shows the voltage and current waveforms of the main components of the converter according to the switching operation of the proposed converter.

As shown in Figure 2, switches S_1 and S_2 operate under soft switching conditions because they switch at zero current or zero voltage at on and off. Looking at the waveform shown in Figure 2, the switch S_2 is always turned on with the internal diode D_2 on, so the zero voltage turn on and off. Switch S_1 is switched on at zero current and off at zero voltage. Also, the internal diode of S_2 does not perform switching operations because the current i_{S1} is always greater than zero because it is in the battery discharge mode. In addition, the internal diode D_2 of the switch S_2 is always zero current turned on and off by the saturation inductor L_S .

Figure 3 shows the operating mode of the proposed converter. The operation mode of the converter according to the switching operation of switches S_1 , S_2 consists of eight modes. The converter operating conditions and analysis results for each mode in Figure 3 are as follows.

When switching, current i_L and output voltage v_o are assumed to be constant current I_L and constant voltage V_o , respectively. In addition, the resonant angular frequency ω_r and characteristic impedance Z of the resonant circuit are as follows.

$$\omega_r = \frac{1}{\sqrt{L_r C_r}} \quad (1)$$

$$Z = \sqrt{\frac{L_r}{C_r}} \quad (2)$$

In Eq.(1) and (2), L_r is the resonant inductance and C_r is the resonant capacitance in Figure 1.

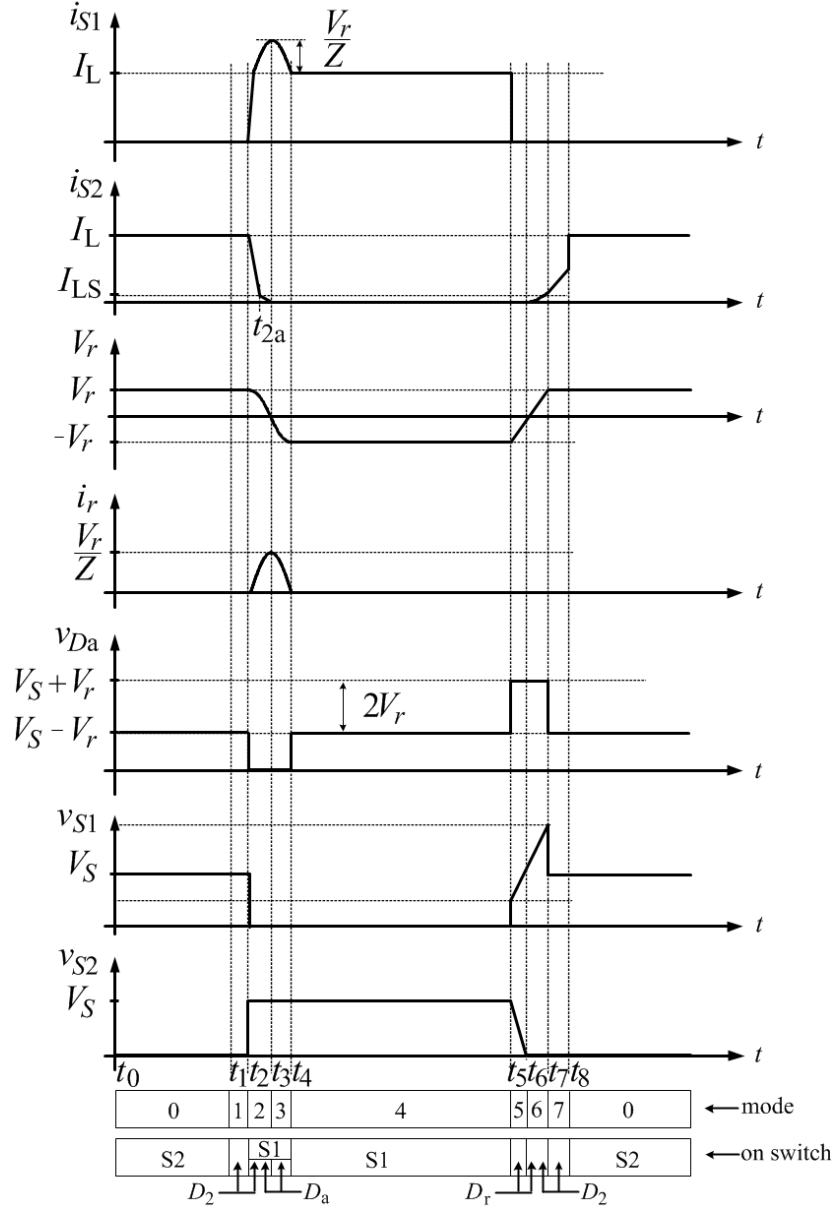


Figure 2. Switching waveforms of proposed converter

Mode 0 ($t_0 \leq t \leq t_1$)

Mode 0 indicates the synchronous mode state in which switch S_2 is turned on. As shown in Figure 3(a), all

other switches remain in turn-off state from t_0 at the start of mode 0 to t_1 at the end of the mode. Therefore, the voltage and current waveforms for each component of the converter retain a constant value as shown in Figure 2. Here, it is assumed that the voltage of capacitor C_r in mode 6 is v_r , and the initial voltage v_r is V_r . If the discharge current is large, the saturated inductor energy is large, so the voltage V_r is the output voltage V_o .

Mode 1 ($t_1 \leq t \leq t_2$)

Mode 1 starts when switch S_2 turns off in mode 1. When switch S_2 is turned off, the current i_L of the inductor L flows through diode D_2 , so the converter operates in mode 1 of Figure 3(b). The voltage and current waveforms for each element of the converter are identical to mode 0 as shown in Figure 2, as diode D_2 is turned on instead of switch S_2 .

Mode 2 ($t_2 \leq t \leq t_3$)

Mode 2 starts when switch S_1 is on in mode 1. When switch S_1 is on, the converter operates in mode 2 in Figure 3(c). As shown in Figure 3(c), V_S voltage is applied to the saturated inductance L_S . Therefore, inductor current i_{S2} is,

$$i_{S2} = I_L - \frac{V_S}{L_{S1}}(t - t_1) \quad (t_2 \leq t \leq t_{2a}) \quad (3)$$

Where $i_{S2}(t_{1a}) = I_{LS}$

When the current i_{S2} of the saturated inductor decreases and the current of L_S is less than the saturation current I_{LS} at t_{2a} , the inductance changes from L_{S1} to L_{S2} . Therefore, i_{S2} is,

$$i_{S2} = I_{LS} - \frac{V_S}{L_{S2}}(t - t_{2a}) \quad (t_{2a} \leq t \leq t_3) \quad (4)$$

In expression (4), mode 2 ends when current i_{S2} reaches 0 at t_3 .

Meanwhile, when mode 2 starts at t_2 , the operation of the resonant circuit ($S_1 - C_r - L_r - D_a$) is shown in Figure 3(c), and inductor current i_r and capacitor voltage v_r are interpreted as follows[8].

$$i_r = \frac{V_r}{Z} \sin[\omega_r(t - t_2)] \quad (5)$$

$$v_r = -V_r \cos[\omega_r(t - t_2)] \quad (6)$$

In Eq.(5) and (6), V_r is the initial voltage v_r . The maximum voltage of v_r is limited to V_S . The resonant frequency $f_r (= \omega_r/2\pi)$ is 10 times higher of converter switching frequency f .

Mode 3 ($t_3 \leq t \leq t_4$)

Even if current i_{S2} is 0 and mode 2 is terminated, the resonant circuit continues to operate as shown in Figure 3(c). Current i_r and voltage v_r are the same as expression (5) and expression (6). Mode 3 terminates when the resonant current i_r reaches zero. In t_4 , where mode 3 terminates, the capacitor voltage $v_r(t_4)$ becomes $-V_r$.

Mode 4 ($t_4 \leq t \leq t_5$)

When the resonant current i_r reaches zero in mode 3, as shown in Figure 3(e), mode 4 starts with only MOSFET S_1 turning on. Mode 4 continues until MOSFET S_1 is switched off.

Mode 5 ($t_5 \leq t \leq t_6$)

Mode 5 starts when switch S_1 is switched off at t_5 . Since the capacitor voltage v_r is $-V_r$ which is less than zero, the inductor current i_r is passed to the output side through capacitor C_r as shown in Figure 3(f). Thus, the capacitor voltage v_r is lowered as follows:

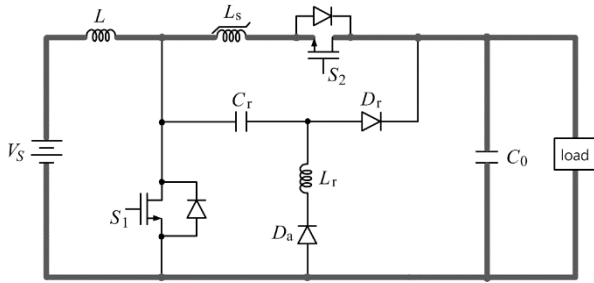
$$v_r = V_r - \frac{L_r}{C_r} t \quad (7)$$

Mode 6 ($t_6 \leq t \leq t_7$)

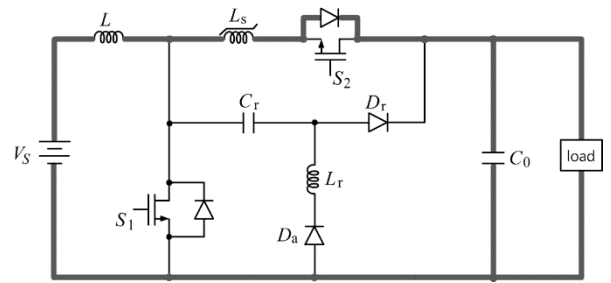
When the capacitor voltage v_r reaches 0V, diode D_2 begins to be turned on, and as shown in Figure 2, the current i_{s2} of the saturated inductor increases gradually. As current i_{s2} gradually increases to I_L , diode D_r is naturally cut off. At the end of mode 6, the capacitor voltage $v_r(t_7)$ depends on $-V_r$, and the voltage V_r depends on the discharge current I_L .

Mode 7 ($t_7 \leq t \leq t_8$)

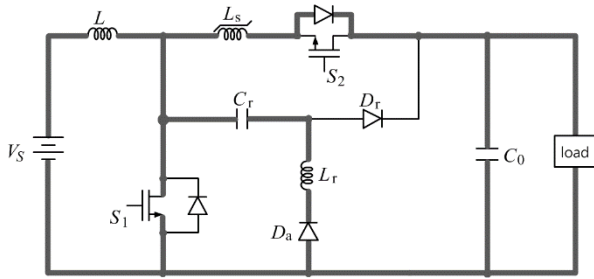
In mode 6, when $i_{s2} = I_L$, the diode D_r is naturally turned off. In mode 7, the converter operates with Figure 3(h). In order to maximize the synchronous mode operating period, mode 7 should reduce the turned on-period between internal diode D_2 as much as possible. Therefore, the time when diode D_2 is turned on is determined by the dead time between switches S_1 and S_2 .



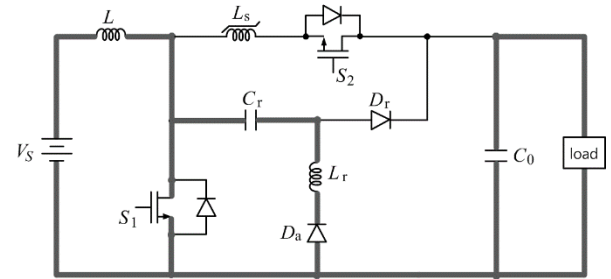
(a) mode 0



(b) mode 1



(c) mode 2



(d) mode 3

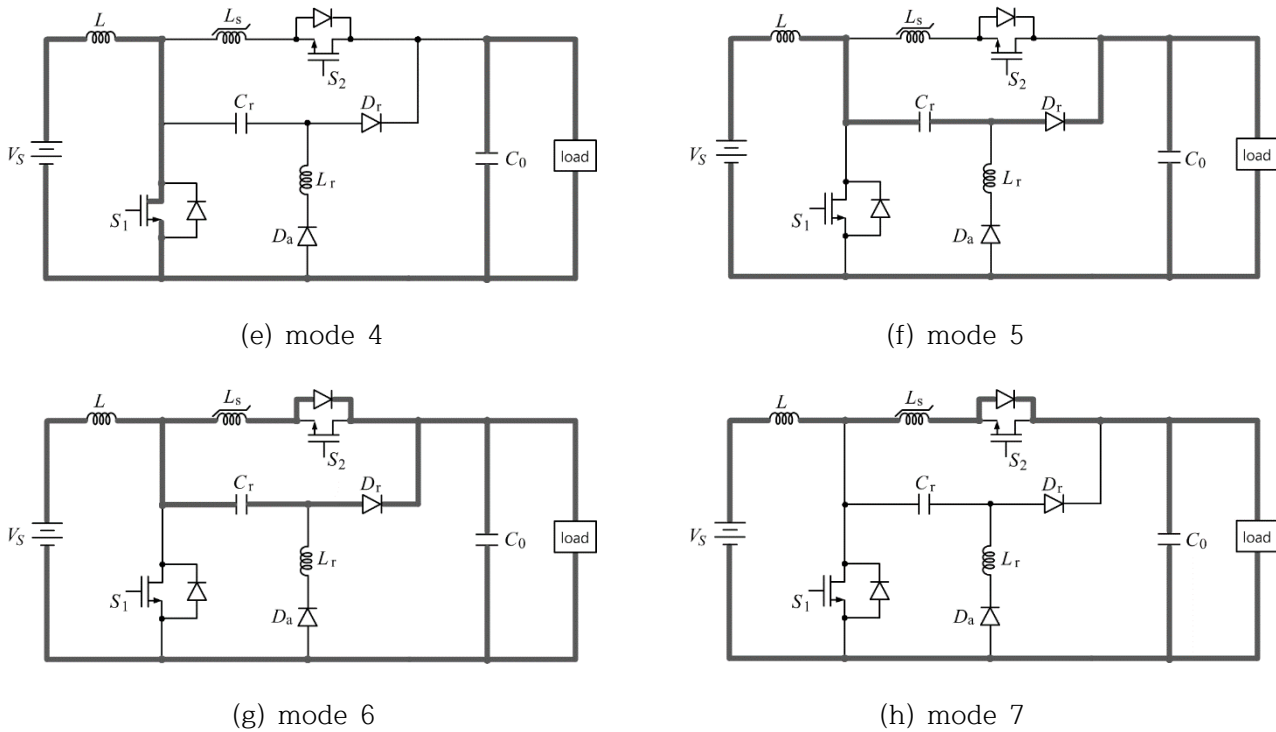


Figure 3. Operating modes of the proposed converter

The switching conditions of switches S_1 and S_2 are summarized in Table 1 as a result of the analysis of the waveform and circuit modes of each part of the converter according to the switching conditions of switches S_1 and S_2 . In Table 1, the main switches S_1 and internal diode D_2 of the converter always perform soft switching operations switching at zero voltage or zero current, also the main switches S_2 of the converter always perform soft switching operations switching at zero voltage.

Table 1. Switch S_1 , S_2 Operating mode

Switch	Switching Operations	
S_1	on \rightarrow off	ZVS (Zero Voltage Switching) low discharging current Partial hard switching
	off \rightarrow on	ZCS (Zero Current Switching)
S_2	on \rightarrow off	ZVS
	off \rightarrow on	ZVS
D_2	on \rightarrow off	ZCS
	off \rightarrow on	ZVS / ZCS

3. Simulations results

Figure 4 is a circuit designed for simulating a battery discharge circuit using PLECS software. In a circuit, the input voltage V_S is 32V and the output voltage is 48V. In Figure 4, the battery current is the average value of the inductor current and the simulation controller is designed to control the battery discharge current, which is the average value of the inductor current.

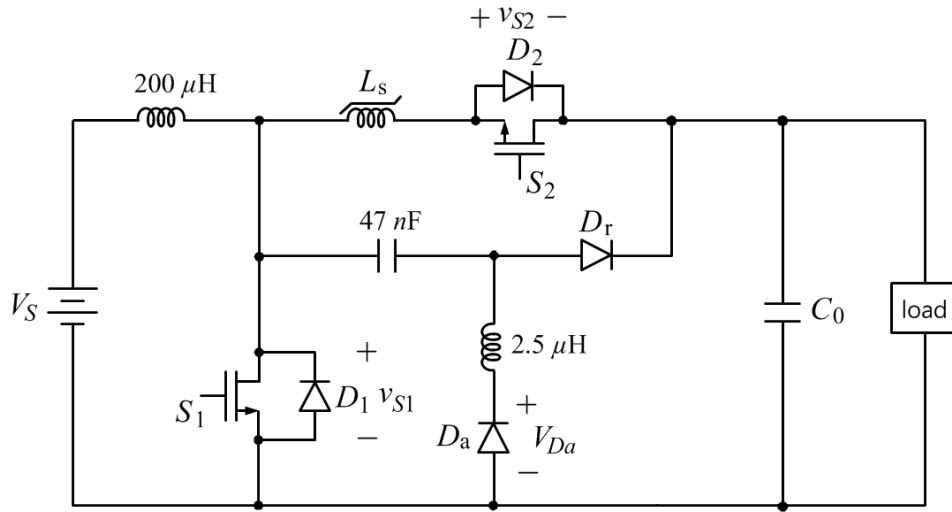


Figure 4. Deigned battery discharger circuit for simulation

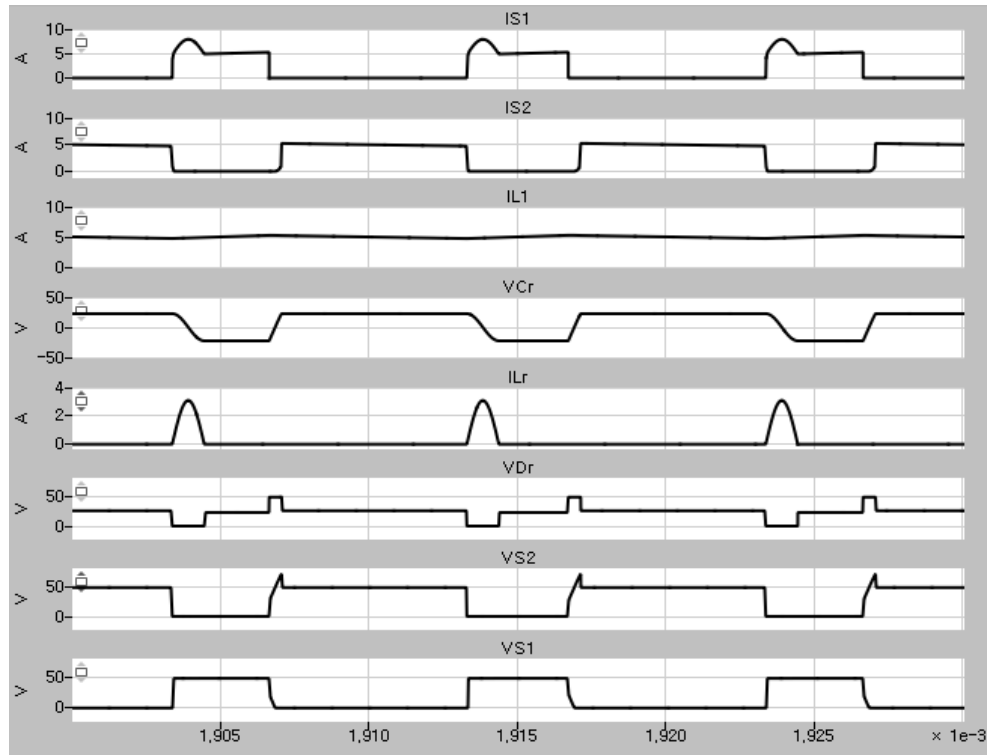


Figure 5. Voltage and current waveforms of battery discharge circuit

Figure 5 shows the voltage and current waveforms for each element of the battery discharge circuit when the battery discharge current is 5 A. Figure 5 shows that the voltage and current of each of the discharge circuit elements are the same characteristics as the waveforms in Figure 2. In the waveform shown in Figure 5, it can be seen that the MOSFET and diode in the circuit mostly perform soft switching operations when on and off.

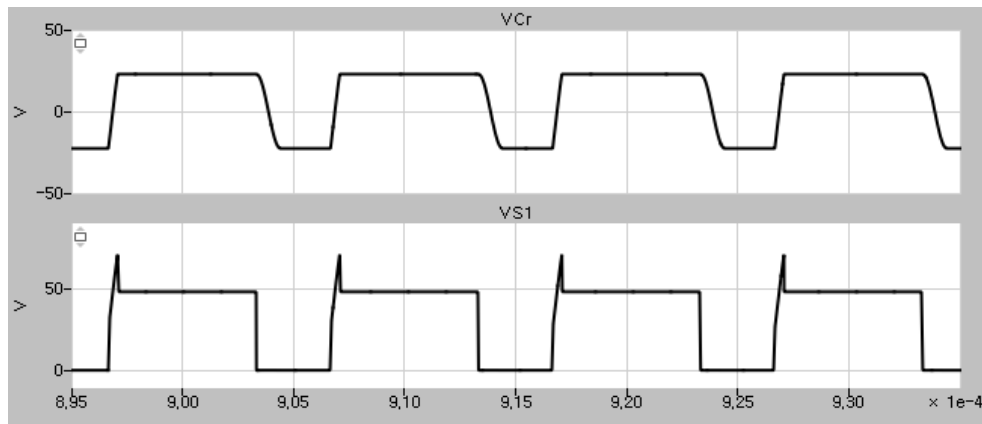


Figure 6. Voltage waveforms of battery discharger circuit for $I_L = 15A$

Figure 6 shows the voltage v_r of the capacitor and the voltage v_{S1} of the MOSFET S_1 when the battery discharge current is 15 A, and as the battery discharge current increases, the energy of the saturated inductance L_{S1} increases, and MOSFET S_1 performs soft switching when the battery discharge current is turned off. In other words, the hard-switching operation that appears when the current is small can be controlled by the inductance value of the saturated inductor.

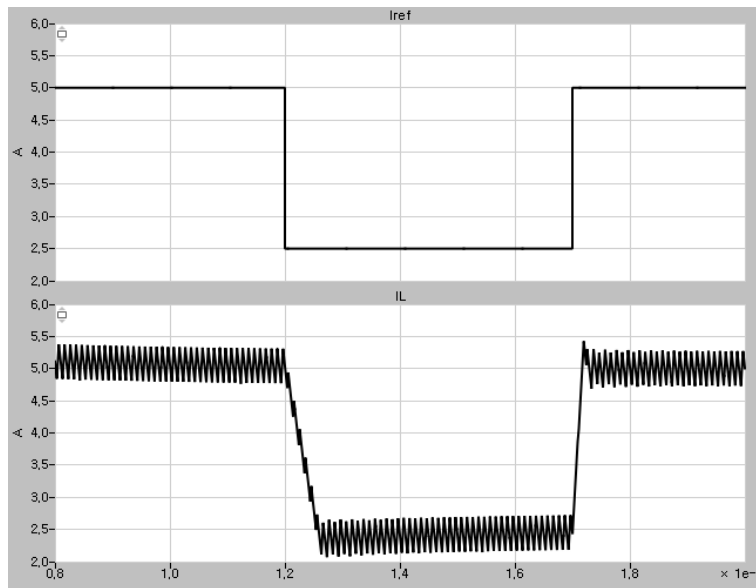


Figure 7. Transient results (I_{REF} : battery reference command, i_L : inductor current)

Figure 7 shows the response characteristics of inductor current i_L , which is a discharge current, when the battery discharge current command current I_{REF} changes. Figure 7 shows that the variation in the battery discharge current of the controller is rapidly controlled within 0.05ms.

4. Conclusions

In this study, a synchronous Boost converter with soft switching for battery discharge was proposed. The

proposed converter has very low switching losses due to its soft switching characteristics. The operation of the converter is synchronous and can be designed to significantly reduce conduction losses. Therefore, switching loss and conduction loss are very low even in the high frequency operation of the converter and have high efficiency characteristics. The high frequency switching operation of the converter also enables the small design of the converter. When most of the weight and volume of the filter composed of inductors and capacitors are reduced in design. By high frequency operation, the compact design of the converter can be achieved. The proposed converter for battery discharge was analyzed, designed and simulated by mode analysis and PLECS simulation. The simulation results demonstrated that the proposed battery discharger operates with soft switching and synchronous characteristics.

Acknowledgement

This research was supported by the Ministry of Trade, Industry & Energy (MOTIE), Korea Agency for Technology and Standards (KATS) for Standard Program – 20006875

References

- [1] Byun Gon Kim, Kwan Woong Kim, Tae Su, Jang, Jun Myung Lee, Yong Kab Kim, " Development of Current Control System for Solar LED Street Light System, " Internal Journal of Advanced Smart Convergence, vol. 1, no. 1, pp. 52-56, May, 2012. <https://doi.org/10.7236/IJASC.2012.1.1.10>
- [2] K. H. Liu, and F. C. Y. Lee, "Zero-voltage switching technique in DC/DC converter, " IEEE Trans. on Power Electronics, vol. 5, no. 3, pp. 293-304, July 1990. <https://doi.org/10.1109/63.56520>
- [3] Gyu Bum Joung, Chun-Tack Rim, Gyu-Heong Cho, " Integral cycle mode control of the series resonant converter, IEEE Transactions on Power Electronics, Vol. 4. No. 1, pp83-91, July, 1989. <https://doi.org/10.1109/63.21875>
- [4] M. R. Mohammadi, H. Farzanehfard, "New family of zero-voltage-transition PWM bidirectional converters with coupled inductors," IEEE Trans. Ind. Electron., Vol. 59, No. 2, pp. 912-919, Feb. 2012. <https://doi.org/10.1109/TIE.2011.2148681>
- [5] E. Adib, and H. Farzanehfard, "Family of Zero-Current Transition PWM Converters, " IEEE Trans. on Industrial Electronics, vol. 55, no. 8, pp. 3055- 3063, August 2008. <https://doi.org/10.1109/TIE.2008.922597>
- [6] P. Das, G. Moschopoulos, "A Comparative Study of ZeroCurrent- Transition PWM Converters", IEEE Trans. on Ind. Electron., Vol. 54, No.3, pp. 1319-1328, 2007. <https://doi.org/10.1109/TIE.2007.891663>
- [7] G. B. Joung, "New Soft Switched PWM Converter," PESC Record. 27th Annual IEEE Power Electronics Specialists Conference, pp. 63-68, June 1996. <https://doi.org/10.1109/PESC.1996.548560>
- [8] Zhiyong Dong, Gyu Bum Joung, "Soft-Switched Synchronous Buck Converter for Battery Chargers," Internal Journal of Advanced Smart Convergence, vol. 8, no. 4, pp. 138-146, Dec 2019. <https://doi.org/10.7236/IJASC.2019.8.4.138>
- [9] I.-D. Kim, J.-Y. Kim, E.-C. Nho, and H.-G. Kim, "Analysis and design of a soft-switched pwm sepic dc-dc converter," Journal of Power Electronics, Vol. 10, No.5, pp.461-467, Sep.2010. <https://doi.org/10.6113/JPE.2010.10.5.461>
- [10] E. Adib and H. Farzanehfard, "Zero-Voltage-Transition PWM Converters With Synchronous Rectifier," IEEE Trans. Power Electronics, vol.25, No. 1, pp. 105-110, Jan. 2010. <https://doi.org/10.1109/TPEL.2009.2024153>